MedChemComm

RESEARCH ARTICLE

View Article Online
View Journal

Cite this: DOI: 10.1039/c8md00484f

Design, synthesis and biological evaluation of tryptamine salicylic acid derivatives as potential antitumor agents†

Runde Xiong,‡[a] Dongxiu He,‡[a] Xiangping Deng,[a] Juan Liu,[a] Xiaoyong Lei,[a] Zhizhong Xie,[a] Xuan Cao,[a] Yanming Chen,[b] Junmei Peng[a] and Guotao Tang *[a]

Received 27th September 2018,
Accepted 5th January 2019

DOI: 10.1039/c8md00484f

rsc.li/medchemcomm

A series of tryptamine salicylic acid derivatives were synthesized and their antiproliferative activity against MGC-803, MCF-7, HepG2, A549 and HeLa cell lines was evaluated. The structure–activity relationship (SAR) study revealed that different substitutions of the C5 and C3′–C5′ positions have certain effects on the anti-proliferation activity. The growth assay revealed that ***N*-[2-(5-bromo-1*H*-indol-3-yl)-ethyl]-2-hydroxy-3-methyl-benzamide** (**E20**) showed the most potent and broad-spectrum anticancer inhibition of all the cell lines evaluated, and was only more potent than 5-Fu for the gastric cancer cell line. Preliminary studies indicated that compound **E20** could inhibit colony formation and migration of MGC-803 cells. The flow cytometry (FCM) results showed that compound **E20** arrested the cell cycle in the G2/M phase and induced apoptosis of MGC-803 cells in a concentration-dependent manner. In addition, the western blot results showed that **E20** can down-regulate the expression of hexokinase 2. Our studies suggest that the framework of ***N*-[2-(5-bromo-1*H*-indol-3-yl)-ethyl]-2-hydroxy-3-methyl-benzamide** may be consider as a new type of chemical for designing effective anti-cancer drugs targeting gastric cancer cells.

1. Introduction

Cancer is a common disease that does great harm to human health. There is an exigent need for high efficiency and low toxicity anticancer drugs that will improve the cure rate of cancer. Melatonin (*N*-acetyl-5-methoxytryptamine) is a kind of indole hormone which is secreted mainly from the pineal gland. However, it is discovered in various other tissues such as the gastrointestinal tract, retina, lens, skin, testes, lymphocytes and hematopoietic cells.[1] As a ubiquitous molecule, melatonin is involved in the regulation of many biological functions[2–5] and protection against a spectrum of cancers such as breast cancer,[6] gastric cancer[7] and liver cancer.[8] Moreover, the mechanisms which have been investigated demonstrated that melatonin could induce cell apoptosis and inhibit proliferation in gastric cancer cells,[9] and western blot analysis showed that melatonin could mediate the upregulation of apoptotic proteins Bax/Bcl-2 and cleaved-caspase 3 in gastric cancer cells.[7] Besides, some researchers reported that melatonin could inhibit aerobic glycolysis (Warburg effect) in human leiomyosarcoma,[10] and others considered it to be an angiogenesis inhibitor which is used to combat cancer.[11] Melatonin showed broad antitumor activities through various mechanisms. Previous studies have focused on the anti-tumor activity of melatonin itself; however, there were fewer studies on the anti-tumor activity of melatonin derivatives.[12–14] This has driven us to transform it into a new anti-tumor agent.

Salicylic acid (SA) and acetylsalicylic acid (ASA) are well known as anti-inflammatory drugs, but they also showed anti-tumor activity,[15] induction of apoptosis[16,17] and modification of tumor glucose utilization.[18] Studies have discovered

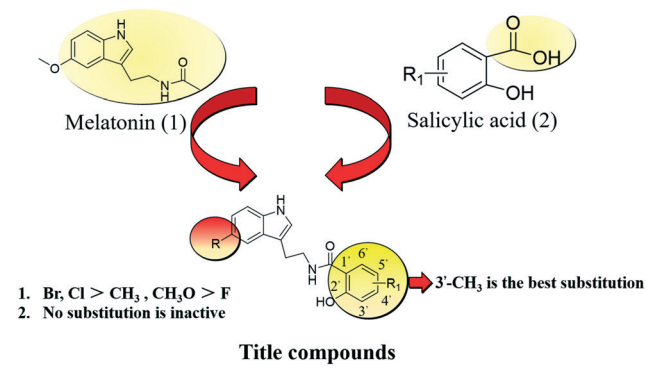

Fig. 1 Design of novel tryptamine salicylic acid derivatives as anti-cancer agents.

[a] Institute of Pharmacy and Pharmacology, Hunan Province Cooperative Innovation Center for Molecular Target New Drug Study, University of South China, Hengyang, China. E-mail: tgtzq@163.com
[b] Jiuzhitang Co. Ltd, Changsha, China

† Electronic supplementary information (ESI) available. See DOI: 10.1039/c8md00484f

‡ These authors contributed equally to this work.

that the anti-tumor activity of SA and ASA was produced by acting on cyclooxygenase (COX)[16,19] and 6-phosphofructo-1-kinase (PFK).[18] SA and ASA could be used as anti-tumor agents.

Although both melatonin and acetylsalicylic acid have antitumor activity, these two drugs show antitumor effects only in the millimolar range.[4,11] In order to obtain a novel small molecular structure with better anti-tumor activity, melatonin is combined with salicylic acid to form new chemotypes, and is modified as shown in Fig. 1. In this study, a series of tryptamine salicylic acid derivatives have been synthesized based on the above structure and evaluated for antitumor activity *in vitro*. Since both have an inhibitory effect on the glycolytic pathway, we investigated whether the most potent drug synthesized (**E20**) has an effect on the expression of three glycolysis-related proteins.

2. Results and discussion

2.1 Chemistry

As shown in Scheme 1, all the compounds were adopted to this synthetic pathway. As shown in Fig. 2, 36 compounds were synthesized and purified by column chromatography. These compounds were obtained in good yields after depuration. All the compounds were characterized by nuclear magnetic resonance-hydrogen spectrum, nuclear magnetic resonance-carbon spectrum and mass spectrometry.

2.2 Antiproliferative activity and SAR discussion

All the compounds were evaluated for their antiproliferative activity in five cell lines namely the human breast cancer cell line (MCF-7), human lung cancer cell line (A549), human liver cancer cell line (HepG2), human gastric cancer cell line (MGC-803) and human cervical cancer cell line (HeLa) by the MTT (3-(4,5-dimethylthiazol-2-yl)-2,5-diphenyltetrazolium bromide) assay.[20] 5-Fu was used as a positive control. As shown in Table 1, most of the synthesized compounds have good antitumor activity, especially on MGC-803 cells. We summed the IC_{50} values of each compound (the IC_{50} value greater than 100 is converted to 100) and made a histogram. It is shown in Fig. 3 that different substituents on C5 had a great effect on the antitumor activity of the compounds, and the different substituents on C3′–C5′ also affected the antitumor activity. According to the histogram, the structure–activity relationship (SAR) of the tryptamine salicylic acid derivatives **E1–E36** was proposed as shown in Fig. 1. The non-substituted compounds on C5 were inactive and the different substitutions on C5 had different activity intensities. Bromine and chlorine had the best activity at the C5 position, followed by methoxy and methyl groups, and finally fluorine. When the same substitution occurred at the C5 position of the compounds, the comparison showed that the methyl substitution of C3′ was the best substitution.

Among these compounds, compound **E20** showed the most potent inhibition of the tested cancer cells with IC_{50} values below 70 μM, but exhibited values greater than that observed for 5-Fu at 50–70 μM. There was one exception – the gastric cancer cell line, MGC-803, which exhibited an IC_{50} of 29 μM (*cf.* 58 μM for 5-Fu). Given the acceptable antiproliferative activity of compound **E20** toward MGC-803 cells, the possible toxicity against the normal human gastric epithelial cell line GES-1 was also preliminarily examined. Compound **E20** showed IC_{50} values of 75 ± 2 μM. It was obvious that the toxicity of **E20** to normal human gastric epithelial cells was significantly lower than that to gastric cancer cells. Because **E20** showed certain selectivity between normal and cancer cells, our studies envisioned that the framework of ***N*-[2-(5-bromo-1*H*-indol-3-yl)-ethyl]-2-hydroxy-3-methyl-benzamide** (**E20**) might be considered as a new type of chemical for designing effective anti-cancer drugs targeting gastric cancer cells. Further structural modifications based on such a scaffold and mechanistic investigations are ongoing in our lab.

We used MOLSOFT online molecular computing service to predict its molecular characteristics (HTTP://MLSOF.COM/).

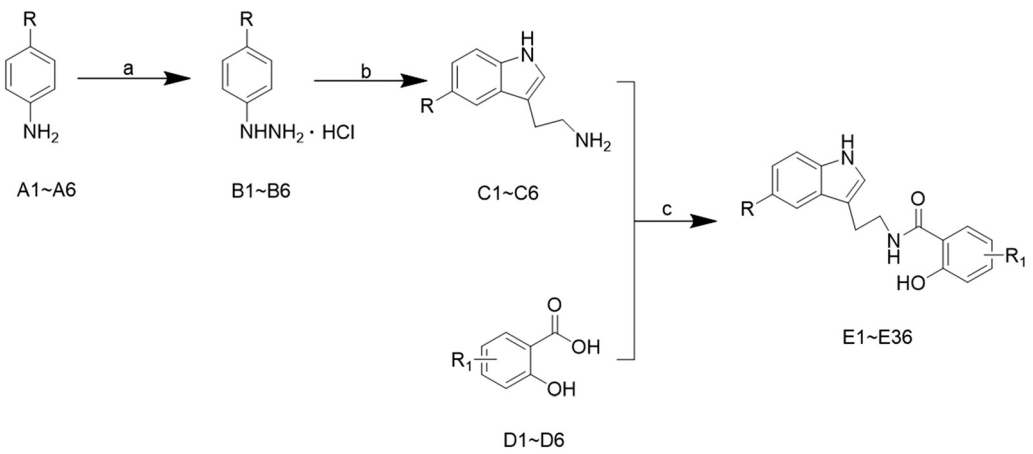

Scheme 1 Reagents and conditions: (a) $NaNO_2$, HCl, Na_2SO_3, reflux 2 h, yield 90–95%; (b) 4-Cl-1-OH-1-butanesulfonate, Na_2HPO_4, CH_3CH_2OH reflux 6 h, yield 50–65%; (c) EDCI, HOBT, acetone, room temperature, yield 70–80%.

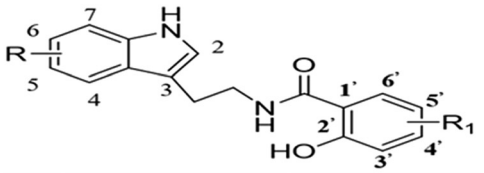

Comp.	R	R_1	Comp.	R	R_1
E1	5-H	/[a]	E19	5-Br	/[a]
E2	5-H	3′ -CH_3	E20	5-Br	3′ -CH_3
E3	5-H	4′ -CH_3	E21	5-Br	4′ -CH_3
E4	5-H	4′ -Cl	E22	5-Br	4′ -Cl
E5	5-H	5′ -Cl	E23	5-Br	5′ -Cl
E6	5-H	5′ -Br	E24	5-Br	5′ -Br
E7	5-Cl	/[a]	E25	5-F	/[a]
E8	5-Cl	3′ -CH_3	E26	5-F	3′ -CH_3
E9	5-Cl	4′ -CH_3	E27	5-F	4′ -CH_3
E10	5-Cl	4′ -Cl	E28	5-F	4′ -Cl
E11	5-Cl	5′ -Cl	E29	5-F	5′ -Cl
E12	5-Cl	5′ -Br	E30	5-F	5′ -Br
E13	5-CH_3	/[a]	E31	5-$CH_3$0	/[a]
E14	5-CH_3	3′ -CH_3	E32	5-$CH_3$0	3′ -CH_3
E15	5-CH_3	4′ -CH_3	E33	5-$CH_3$0	4′ -CH_3
E16	5-CH_3	4′ -Cl	E34	5-$CH_3$0	4′ -Cl
E17	5-CH_3	5′ -Cl	E35	5-$CH_3$0	5′ -Cl
E18	5-CH_3	5′ -Br	E36	5-$CH_3$0	5′ -Br

[a] "/" represents none.

Fig. 2 The tryptamine salicylic acid derivatives with different substituents.

As shown in Table 2, compound **E20** showed acceptable molecular properties and might have acceptable pharmacokinetic properties.

2.3 Colony formation assay of E20 on MGC-803 cells

To prove the anti-proliferative activity of compound **E20**, the colony formation assay was used to test the effect of compound **E20** on MGC-803 cells. Cells were treated with different concentrations (10, 20 and 40 μM) of **E20**. As shown in Fig. 4A, the treatment of **E20** significantly reduced the number of viable cells in a concentration-dependent manner compared to the DMSO-treated group, and the cells were completely killed at 40 μM.

2.4 E20 can inhibit the migration of MGC-803 cells

The strong ability of migration of cancer cells plays an important role in the mortality and prognosis of cancer patients;[21,22] so we further studied the effect of **E20** on cell migration activity using the wound healing assay. We scratched the cells within each well with a 200 μL sterile pipette tip, removed the floating cells by rinsing with PBS, and treated the remaining cells with different concentrations of **E20** for 48 h. The control group was treated with 3‰ DMSO for 48 h. We captured images of the cells with a microscopic camera system at the time of treatment (0 h) and after 48 h to assess the re-growth of the colony back into the damaged region. As shown in Fig. 4B, the wounded area was almost completely healed in the DMSO-treated control after 48 h, while compound **E20** inhibited the healing of the wounded area in a concentration-dependent manner.

2.5 Effect of compound E20 on apoptosis in MGC-803 cells

Flow cytometry was used to analyze the cells. MGC-803 cells were treated with compound **E20** and the Annexin V-FITC/propidium iodide (PI) double staining assay (BD Pharmingen, USA)[23] was used. MGC-803 cells were treated with different concentrations (10, 20, and 30 μM) of **E20** for 48 h and the control group was treated with 3‰ DMSO, then stained with Annexin V-FITC and propidium iodide. The stained cells were analyzed using a flow cytometer. As shown in Fig. 5, the percentage of apoptosis in the treated group was higher than that in the control group, and compound **E20** induced apoptosis of MGC-803 cells in a concentration-dependent manner.

2.6 Effect of compound E20 on the cell cycle in MGC-803 cells

To demonstrate the effect of compound **E20** on the cell cycle, we used flow cytometry for analysis. MGC-803 cells were treated with compound **E20** (20, 40, and 60 μM) and the control group was treated with 3‰ DMSO, then mixed with propidium iodide (PI) staining solution and RNase A. As

Table 1 IC_{50} (μM) of analogues against different cell lines

Compounds	$IC_{50} \pm SD^a$ (μM)				
	MCF-7	A549	MGC-803	HepG2	HeLa
E1	>100	>100	>100	>100	>100
E2	>100	>100	63 ± 3	>100	82 ± 2
E3	>100	>100	80 ± 4	>100	>100
E4	>100	>100	80 ± 3	>100	>100
E5	>100	>100	74 ± 5	>100	>100
E6	>100	>100	78 ± 5	>100	>100
E7	75 ± 2	60 ± 3	35 ± 5	>100	81 ± 2
E8	70 ± 4	48 ± 3	56 ± 5	62 ± 2	56 ± 3
E9	73 ± 2	63 ± 1	37 ± 5	>100	64 ± 1
E10	69 ± 3	46 ± 6	34 ± 3	90 ± 1	64 ± 2
E11	80 ± 2	62 ± 1	31 ± 6	89 ± 5	80 ± 3
E12	75 ± 4	63 ± 4	35 ± 6	>100	85 ± 6
E13	93 ± 4	>100	45 ± 5	>100	>100
E14	62 ± 3	50 ± 1	38 ± 3	64 ± 5	61 ± 3
E15	60 ± 2	75 ± 3	38 ± 4	>100	>100
E16	>100	68 ± 1	47 ± 4	98 ± 6	93 ± 4
E17	79 ± 2	89 ± 4	42 ± 2	>100	>100
E18	89 ± 3	80 ± 3	61 ± 1	93 ± 5	>100
E19	80 ± 2	59 ± 4	37 ± 3	>100	79 ± 5
E20	63 ± 1	36 ± 3	29 ± 3	45 ± 5	52 ± 2
E21	80 ± 5	61 ± 1	48 ± 6	80 ± 6	61 ± 3
E22	98 ± 5	63 ± 3	43 ± 5	92 ± 6	71 ± 2
E23	73 ± 4	63 ± 3	63 ± 6	87 ± 5	80 ± 3
E24	>100	62 ± 4	80 ± 4	>100	>100
E25	>100	>100	63 ± 1	>100	>100
E26	>100	67 ± 4	52 ± 4	>100	>100
E27	>100	>100	60 ± 3	>100	>100
E28	>100	>100	62 ± 3	>100	>100
E29	>100	53 ± 4	53 ± 6	>100	>100
E30	>100	77 ± 3	80 ± 3	>100	76 ± 3
E31	>100	>100	59 ± 3	>100	82 ± 3
E32	97 ± 4	>100	43 ± 1	85 ± 2	42 ± 3
E33	>100	>100	59 ± 2	80 ± 1	80 ± 3
E34	>100	>100	56 ± 3	>100	71 ± 5
E35	>100	>100	55 ± 1	75 ± 3	>100
E36	>100	>100	62 ± 2	>100	74 ± 4
5-Fu	57 ± 3	>100	58 ± 1	68 ± 8	50 ± 7

[a] Data are the average of three independent assays; SD: standard deviation.

shown in Fig. 6, the percentage of cells in the G0/G1, S and G2/M phase was obtained with flow cytometry. Compound **E20** caused accumulation of cells in the G2/M phase of the cell cycle and the shift to this phase was stronger with increasing concentration of **E20**.

2.7 E20 inhibited the expression of HK2

It has been reported that the anti-tumor effects of melatonin and salicylic acid are related to glycolysis-related proteins, and representative proteins are hypoxia-inducible factor-1α (HIF-1α), hexokinase 2 (HK2) and phosphofructokinase (PFK).[24] Compound **E20** was a modified structure based on the combination of melatonin and salicylic acid. According to the combination principles, it is likely that **E20** also inhibited glycolysis by inhibiting the above-related proteins. To further investigate whether the anti-proliferative effect of compound **E20** on gastric cancer cells is related to the relevant anti-tumor targets, we performed western blot experiments on the above three proteins. As shown in Fig. 7, compound **E20** had no effect on HIF-1 and PFK but down-regulated the expression of HK2.

3. Conclusion

In summary, a new class of tryptamine salicylic acid derivatives was synthesized and evaluated against MGC-803, MCF-7, A549, HepG2 and HeLa cell lines. The MTT assay revealed that compound **E20** was the most potent, showed broad-spectrum anticancer inhibition against all the evaluated cell lines, and was especially sensitive to the MGC-803 cell line. Our preliminary observations indicated that compound **E20**, when added to MGC-803 cells: (1) inhibited colony formation and migration; (2) induced apoptosis in a concentration-dependent manner; (3) inhibited their growth by blocking the G2/M phase of the cell cycle; and (4) down-regulated the expression of HK2. Our studies envisioned that the framework of ***N*-[2-(5-bromo-1*H*-indol-3-yl)-ethyl]-2-hydroxy-3-methyl-benzamide** (**E20**) might be considered as a new type of chemical for designing effective anti-cancer drugs targeting gastric cancer cells.

4. Experimental section

4.1 Chemical synthesis

All chemicals (reagent grade) were purchased from Aladdin-Reagent Co., Ltd (China) and used without further purification unless otherwise stated. Melting points (uncorrected) were determined on a Thermo Scientific electrothermal digital melting point apparatus. ESI mass spectra were obtained on a Waters GCT mass spectrometer, and ^{1}H NMR spectra were measured on a Bruker AV-400 model spectrometer with TMS and solvent signals slotted as internal standards. Chemical shifts were reported in ppm (δ).

4.1.1 Synthetic procedure for the synthesis of B1–B6. A stirred solution of aniline (2.80 g, 0.03 mol) in 12% hydrochloric acid solution (27 mL) was cooled to 0–5 °C. Then a sodium nitrite solution (2.16 g, 0.031 mol) was added dropwise and reacted for 1 h. After the reaction was completed, the solution was added to an aqueous solution of sodium sulfite (11.34 g, 0.09 mol) at room temperature and then heated to 80 °C. After 2 h, concentrated hydrochloric acid (6 mL) was added and the reaction was stirred at 100 °C for 2 h. After cooling to room temperature, phenylhydrazine hydrochloride (**B1**) was precipitated from the solution. Compounds **B2–B6** were prepared in a similar way. Yields: 90–95%.

4.1.2 Synthetic procedure for the synthesis of C1–C6. To a solution of **B1** (2.90 g, 0.02 mol) in 30% ethanol solution were added 4-chloro-1-hydroxy-1-butanesulfonate sodium (4.21 g, 0.02 mol) and Na_2HPO_4 (0.14 g, 0.001 mol), the mixture was stirred at 70 °C for 6 h. After evaporating the ethanol, the mixture was washed with dichloromethane and chloroform, then the pH was adjusted to 7 with saturated sodium bicarbonate and the mixture was cooled to 4 °C, during

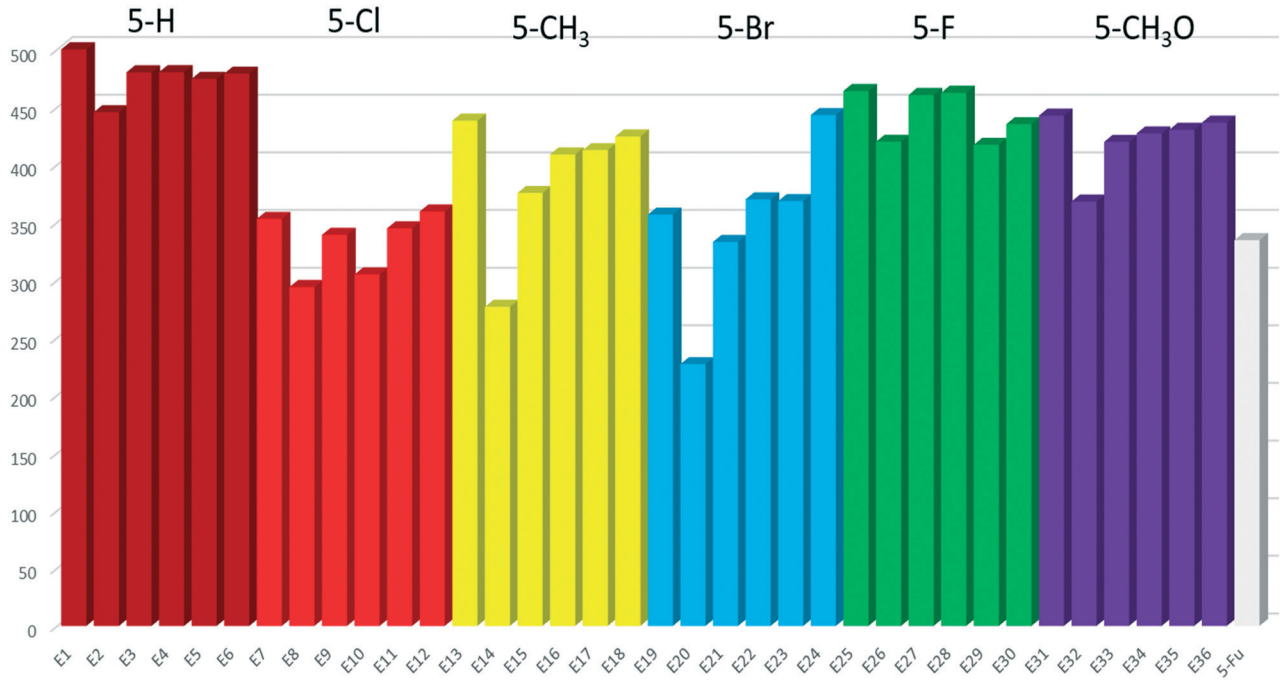

Fig. 3 The ordinate axis represents the sum of the IC_{50} values of the five cell lines and the abscissa axis represents different compounds. We can more intuitively observe the structure–activity relationship of tryptamine salicylic acid derivatives.

Table 2 Molecular properties of **E20**[a]

Compound	MW	HBA	HBD	MolLogP	MolPSA (A^2)	MV (A^3)
Desirable value	<500	<10	<5	<5	<140	—
E20	372.05	2	3	4.05	49.84	318.79

[a] MW: molecular weight; HBA: number of hydrogen bond acceptors; HBD: number of hydrogen bond donors; MolLogP: log*p* value predicted by Molsoft; MolPSA: polar surface area; MV: molecular volume.

which **C1** was precipitated from the solution. After filtration, the product was used in the next step without purification. Compounds **C2–C6** were prepared in a similar way. Yields: 50–65%.

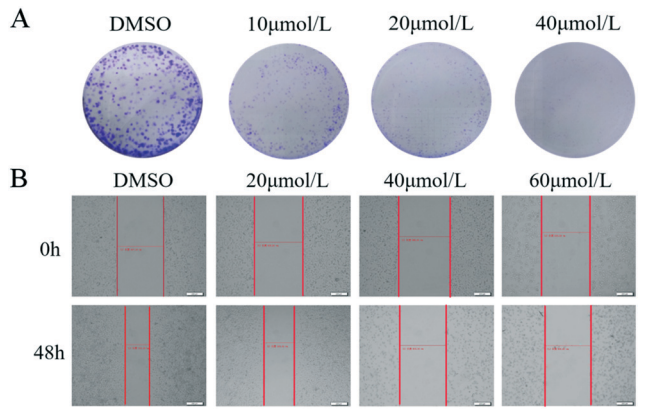

Fig. 4 (A) **E20** inhibited the growth and migration of MGC-803 cells. Representative images of MGC-803 cell colonies after treatment with **E20** at different concentrations for 9 days. (B) Wound healing assay.

4.1.3 Synthetic procedure for the synthesis of E1–E36. To a solution of salicylic acid (0.14 g, 0.001 mol) in acetone (15.0 ml) were added EDCI (0.573 g, 0.003 mol) and HOBt (0.405 g, 0.003 mol) at room temperature. After 4 h, compound **E1** was added and the reaction mixture was stirred at room temperature for 24 h. The crude product purified by silica gel column chromatography (petroleum ether/EtOAc = 2 : 1) to obtain the final product.

2-Hydroxy-N-[2-(1H-indol-3-yl)-ethyl]-benzamide (E1). Yellow-white powder, 80.53% yield, mp 154–156 °C; ^{1}H NMR (400 MHz, $CDCl_3$) δ 12.41 (s, 1H), 8.20 (s, 1H,), 7.62 (s, 1H), 7.39 (t, J = 7.6 Hz, 1H), 7.33 (d, J = 8.5 Hz, 1H), 7.29 (s, 1H), 7.21 (s, 1H), 7.19 (s, 1H), 7.12 (s, 1H), 7.01 (d, J = 8.3 Hz, 1H), 6.81 (t, J = 7.3 Hz, 1H), 6.44 (s, 1H), 3.79 (d, J = 5.7 Hz, 2H), 3.08 (t, J = 6.2 Hz, 2H); ^{13}C NMR (101 MHz, acetone) δ 170.66 (s), 160.25 (s), 135.26 (s), 134.35 (s), 127.97 (s), 127.35 (s), 126.60 (s), 123.90 (s), 122.88 (s), 122.67 (s), 118.13 (s), 117.56 (s), 113.81 (s), 111.86 (s), 111.02 (s), 40.33 (s), 25.08 (s). MS (ESI): 280.32 ($C_{17}H_{16}N_2O_2$, [M + H^+]).

2-Hydroxy-N-[2-(1H-indol-3-yl)-ethyl]-3-methyl-benzamide (E2). White powder, 80.53% yield, mp 165–167 °C; ^{1}H NMR (400 MHz, $CDCl_3$) δ 12.39 (s, 1H), 8.22 (s, 1H), 7.61 (s, 1H),

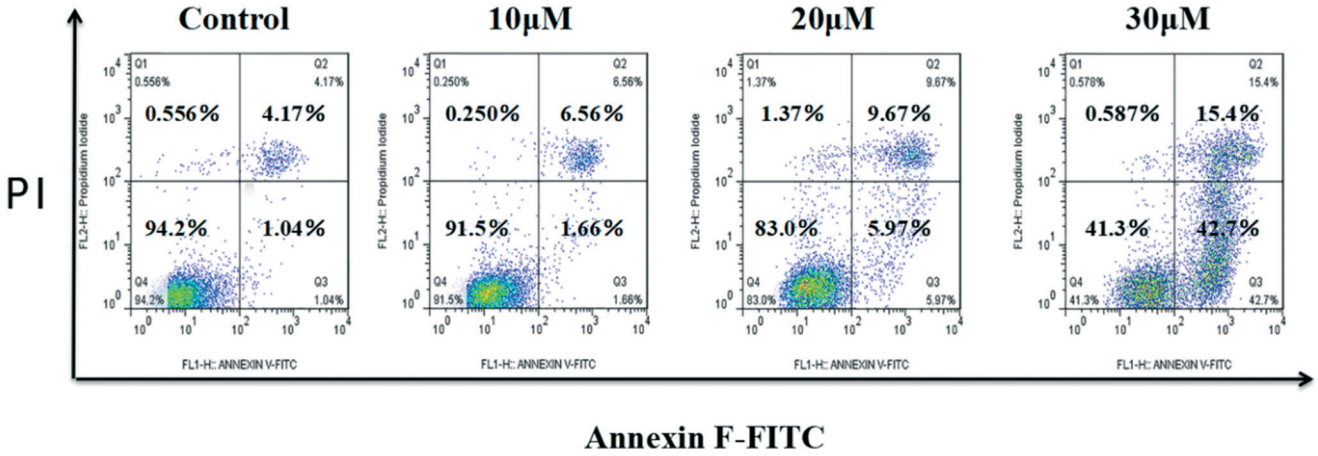

Fig. 5 Apoptotic effect of **E20** on MGC-803 cells after treatment for 48 h. The lower left quadrant represents live cells, the lower right is for early/primary apoptotic cells, the upper right is for late/secondary apoptotic cells, and the upper left represents cells damaged during the procedure.

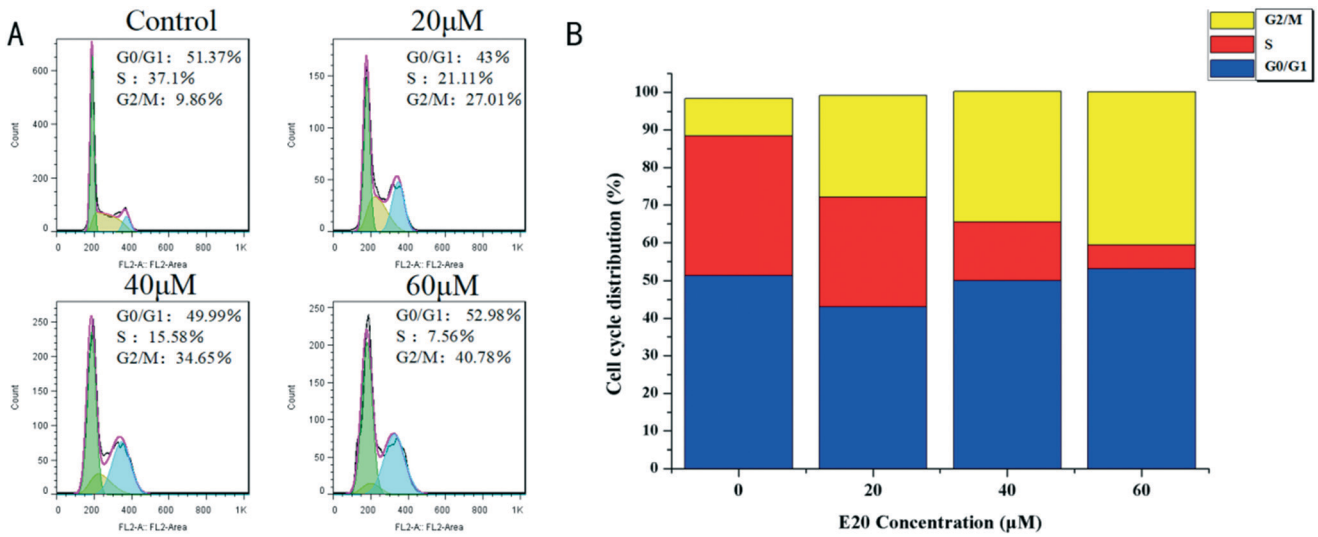

Fig. 6 Effect of **E20** on cell cycle progression in MGC-803 cells. (A) Cells were treated with different concentrations of **E20** for 24 h, then the cell cycle distribution was analysed by flow cytometry. (B) Graph reporting percentile cell-cycle phase distributions. G0/G1, S and G2/M phase distributions were determined by FlowJo analysis.

7.33 (d, J = 8.5 Hz, 1H), 7.29 (s, 1H), 7.20 (d, J = 7.9 Hz, 1H), 7.11 (s, 1H), 7.08 (d, J = 7.8 Hz, 1H), 6.82 (s, 1H), 6.62 (d, J = 7.3 Hz, 1H), 6.37 (s, 1H), 3.77 (d, J = 5.1 Hz, 2H), 3.07 (d, J = 5.9 Hz, 2H), 2.33 (s, 3H); ^{13}C NMR (101 MHz, acetone) δ 170.69 (s), 160.25 (s), 136.88 (s), 134.40 (s), 127.69 (s), 126.63 (s), 123.91 (s), 122.58 (s), 121.32 (s), 118.64 (s), 118.43 (s), 117.59 (s), 113.79 (s), 112.33 (s), 111.34 (s), 40.22 (s), 25.13 (s), 14.92 (s). MS (ESI): 294.35 ($C_{18}H_{18}N_2O_2$, [M + H$^+$]).

2-Hydroxy-N-[2-(1H-indol-3-yl)-ethyl]-4-methyl-benzamide (E3). White powder, 82.63% yield, mp 164–167 °C. ^{1}H NMR (400 MHz, $CDCl_3$) δ 12.72 (s, 1H), 8.02 (s, 1H), 7.43 (s, 1H), 7.31 (d, J = 8.3 Hz, 1H), 7.29 (s, 1H), 7.25 (d, J = 7.2 Hz, 1H), 7.10 (s, 1H), 7.07 (s, 1H), 6.97 (d, J = 7.9 Hz, 1H), 6.67 (t, J = 7.6 Hz, 1H), 6.42 (s, 1H), 3.83–3.73 (m, 2H), 3.10 (t, J = 6.3 Hz, 2H), 2.46 (s, 3H); ^{13}C NMR (101 MHz, acetone) δ 170.68 (s), 160.26 (s), 136.88 (s), 134.39 (s), 127.69 (s), 126.63 (s), 123.91 (s), 122.58 (s), 121.31 (s), 118.62 (s), 118.42 (s), 117.58 (s), 113.79 (s), 112.32 (s), 111.33 (s), 40.21 (s), 25.13 (s), 14.90 (s). MS (ESI): 294.35 ($C_{18}H_{18}N_2O_2$, [M + H$^+$]).

4-Chloro-2-hydroxy-N-[2-(1H-indol-3-yl)-ethyl]-benzamide (E4). White powder, 84.53% yield, mp 158–160 °C. ^{1}H NMR (400 MHz, $CDCl_3$) δ 12.55 (s, 1H), 8.12 (s, 1H), 7.51 (s, 1H), 7.22 (d, J = 8.6 Hz, 1H), 7.18 (s, 1H), 7.16 (d, J = 7.3 Hz, 1H), 7.09 (d, J = 8.6 Hz, 1H), 7.01 (s, 1H), 6.94 (d, J = 7.9 Hz, 1H), 6.60 (t, J = 7.6 Hz, 1H), 6.32 (s, 1H), 3.67 (q, J = 6.0 Hz, 2H), 2.96 (t, J = 6.5 Hz, 2H); ^{13}C NMR (101 MHz, acetone) δ 169.51 (s), 162.72 (s), 138.59 (s), 136.88 (s), 128.04 (s), 127.66 (s), 122.61 (s), 121.32 (s), 118.74–118.28 (m), 117.56 (s), 113.60 (s), 112.20 (s), 111.35 (s), 40.27 (s), 25.01 (s). MS (ESI): 314.77 ($C_{17}H_{15}ClN_2O_2$, [M + H$^+$]).

5-Chloro-2-hydroxy-N-[2-(1H-indol-3-yl)-ethyl]-benzamide (E5). White powder, 74.56% yield, mp 170–173 °C. ^{1}H NMR (400 MHz, $CDCl_3$) δ 12.35 (s, 1H), 8.20 (s, 1H), 7.60 (s, 1H), 7.46 (d, J = 8.8 Hz, 1H), 7.33 (d, J = 8.6 Hz, 1H), 7.28 (s, 1H),

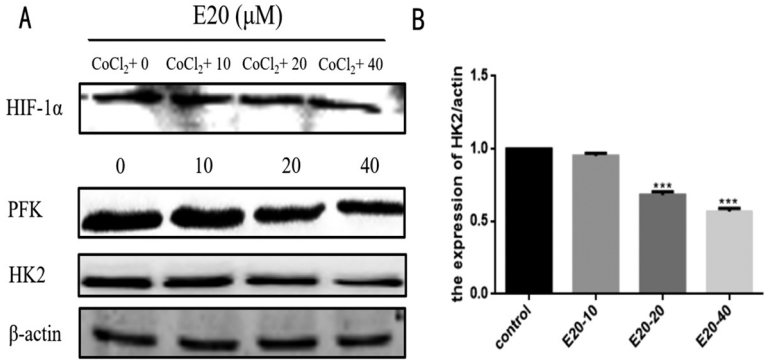

Fig. 7 Western blot analysis of **E20** in MGC3-803 cells. Cells were cultured in the presence of different concentrations of **E20** (μM) for 24 h. (A) The expression of HIF-1α, HK2 and PFK proteins. The expression of HIF-1α required the addition of $CoCl_2$ (100 μM) to produce hypoxic conditions. Representative photographs from three independent experiments are shown. (B) **E20** only inhibited the expression of HK2, but had no obvious effect on PFK and HIF-1α. Western blot results of the HK2 protein were selected for statistical analysis. Quantification of the western blot result was conducted by calculating the ratio of the value to the control group. *$p < 0.05$, **$p < 0.01$, ***$p < 0.001$ *vs.* control.

7.25(d, J = 7.3 Hz, 1H), 7.21 (d, J = 8.6 Hz, 1H), 7.12 (s, 1H), 6.90 (d, J = 8.8 Hz, 1H), 6.38 (s, 1H), 3.77 (q, J = 6.4 Hz, 2H), 3.07 (t, J = 6.6 Hz, 2H). ^{13}C NMR (101 MHz, acetone) δ 169.02 (s), 160.50 (s), 136.87 (s), 133.47 (s), 127.66 (s), 126.18 (s), 122.58 (d, J = 8.3 Hz), 121.31 (s), 119.57 (s), 118.63 (s), 118.37 (s), 115.83 (s), 112.18 (s), 111.34 (s), 40.35 (s), 24.96 (s). MS (ESI): 314.77 ($C_{17}H_{15}ClN_2O_2$, [M + H^+]).

5-Bromo-2-hydroxy-N-[2-(1H-indol-3-yl)-ethyl]-benzamide (E6). White powder, 75.56% yield, mp 174–177 °C. ^{1}H NMR (400 MHz, $CDCl_3$) δ 12.40 (s, 1H), 8.15 (s, 1H), 7.67 (d, J = 7.8 Hz, 1H), 7.46 (s, 1H), 7.44 (s, 1H), 7.27 (s, 1H), 7.23 (s, 1H), 7.20 (d, J = 7.4 Hz, 1H), 7.12 (s, 1H), 6.90 (d, J = 8.8 Hz, 1H), 6.36 (s, 1H), 3.92–3.68 (m, 2H), 3.13 (t, J = 6.5 Hz, 2H). ^{13}C NMR (101 MHz, DMSO) δ 167.83 (s), 159.51 (s), 136.72 (s), 136.46 (s), 130.57 (s), 127.63 (s), 123.22 (s), 121.43 (s), 120.21 (s), 118.71 (d, J = 6.4 Hz), 117.83 (s), 111.92 (d, J = 7.2 Hz), 110.14 (s), 25.23 (s). MS (ESI): 359.22 ($C_{17}H_{15}BrN_2O_2$, [M + H^+]).

N-[2-(5-Chloro-1H-indol-3-yl)-ethyl]-2-hydroxy-benzamide (E7). White-brown powder, 78.46% yield, mp 132–137 °C. ^{1}H NMR (400 MHz, $CDCl_3$) δ 12.41 (s, 1H), 8.18 (s, 1H), 7.62 (d, J = 1.9 Hz, 1H), 7.40 (ddd, J = 8.6, 7.3, 1.5 Hz, 1H), 7.33 (d, J = 8.6 Hz, 1H), 7.22–7.17 (m, 2H), 7.13 (d, J = 2.2 Hz, 1H), 7.00 (dd, J = 8.4, 1.0 Hz, 1H), 6.83–6.78 (m, 1H), 6.41 (s, 1H), 3.79 (dd, J = 12.6, 6.6 Hz, 2H), 3.08 (t, J = 6.7 Hz, 2H); ^{13}C NMR (101 MHz, acetone) δ 170.23 (s), 161.86 (s), 135.25 (s), 133.75 (s), 128.85 (s), 126.47 (s), 124.53 (s), 124.03 (s), 121.31 (s), 118.27 (s), 117.83 (d, J = 4.6 Hz), 114.67 (s), 112.72 (s), 112.29 (s), 40.07 (s), 24.88 (s). MS (ESI): 314.77 ($C_{17}H_{15}ClN_2O_2$, [M + H^+]).

N-[2-(5-Chloro-1H-indol-3-yl)-ethyl]-2-hydroxy-3-methyl-benzamide (E8). Brown powder, 80.46% yield, mp 174–176 °C. ^{1}H NMR (400 MHz, $CDCl_3$) δ 12.65 (s, 1H), 8.15 (s, 1H), 7.62 (d, J = 2.0 Hz, 1H), 7.35–7.32 (m, 1H), 7.26 (d, J = 7.3 Hz, 1H), 7.20 (dd, J = 8.6, 2.0 Hz, 1H), 7.13 (d, J = 2.3 Hz, 1H), 7.05–7.01 (m, 1H), 6.71 (dd, J = 9.5, 5.8 Hz, 1H), 6.39 (s, 1H), 3.78 (dd, J = 12.6, 6.6 Hz, 2H), 3.08 (q, J = 6.4 Hz, 2H), 2.29 (s, 3H). ^{13}C NMR (101 MHz, acetone) δ 170.70 (s), 160.23 (s), 135.25 (s), 134.39 (s), 128.86 (s), 126.62 (s), 124.53 (s), 123.95 (d, J = 14.7 Hz), 121.31 (s), 117.85 (s), 117.60 (s), 113.75 (s), 112.72 (s), 112.30 (s), 40.09 (s), 24.90 (s), 14.87 (s). MS (ESI): 328.79 ($C_{18}H_{17}ClN_2O_2$, [M + H^+]).

N-[2-(5-Chloro-1H-indol-3-yl)-ethyl]-2-hydroxy-4-methyl-benzamide (E9). Brown powder, 80.46% yield, mp 174–176 °C. ^{1}H NMR (400 MHz, DMSO) δ 12.60 (s, 1H), 11.08 (s, 1H), 8.87 (t, J = 5.6 Hz, 1H), 7.77 (d, J = 1.8 Hz, 1H), 7.75 (d, J = 8.4 Hz, 1H), 7.31 (d, J = 8.6 Hz, 1H), 7.26 (d, J = 2.2 Hz, 1H), 7.20 (dd, J = 8.6, 1.9 Hz, 1H), 6.70 (s, 1H), 6.73 (s, 1H), 3.51 (dd, J = 13.3, 7.1 Hz, 2H), 2.98 (t, J = 7.3 Hz, 2H), 2.29 (s, 3H); ^{13}C NMR (101 MHz, acetone) δ 170.27 (s), 161.93 (s), 144.57 (s), 135.25 (s), 128.86 (s), 126.30 (s), 124.51 (s), 124.03 (s), 121.31 (s), 119.35 (s), 117.91 (d, J = 9.1 Hz), 112.72 (s),112.21 (d, J = 26.4 Hz), 39.99 (s), 24.94 (s), 20.61 (s). MS (ESI): 328.79 ($C_{18}H_{17}ClN_2O_2$, [M + H^+]).

4-Chloro-N-[2-(5-chloro-1H-indol-3-yl)-ethyl]-2-hydroxy-benzamide (E10). White powder, 78.47% yield, mp 140–144 °C. ^{1}H NMR (400 MHz, DMSO) δ 12.91 (s, 1H), 11.05 (s, 1H), 8.96 (t, J = 5.4 Hz, 1H′), 7.85 (d, J = 8.4 Hz, 1H), 7.61 (d, J = 1.7 Hz, 1H), 7.36 (d, J = 8.6 Hz, 1H), 7.27 (d, J = 2.0 Hz, 1H), 7.06 (dd, J = 8.6, 2.0 Hz, 1H), 6.99 (dd, J = 3.3, 2.0 Hz, 1H), 6.97–6.95 (m, 1H), 3.55 (dd, J = 13.2, 6.9 Hz, 2H), 2.95 (t, J = 7.3 Hz, 2H); ^{13}C NMR (101 MHz, DMSO) δ 168.35 (s), 161.16 (s), 137.98 (s), 135.16 (s), 129.93 (s), 128.84 (s), 125.20 (s), 123.52 (s), 121.34 (s), 119.29 (s), 118.05 (s), 117.46 (s), 115.04 (s), 113.40 (s), 112.04 (s), 25.05 (s). MS (ESI): 349.21 ($C_{17}H_{14}Cl_2N_2O_2$, [M + H^+]).

5-Chloro-N-[2-(5-chloro-1H-indol-3-yl)-ethyl]-2-hydroxy-benzamide (E11). White powder, 75.47% yield, mp 164–165 °C. ^{1}H NMR (400 MHz, DMSO) δ 12.61 (s, 1H), 11.05 (s, 1H), 8.99 (t, J = 5.5 Hz, 1H), 7.92 (d, J = 2.6 Hz, 1H), 7.61 (d, J = 2.0 Hz, 1H), 7.43 (dd, J = 8.8, 2.6 Hz, 1H), 7.36 (d, J = 8.6 Hz, 1H), 7.28 (d, J = 2.2 Hz, 1), 7.06 (dd, J = 8.6, 2.0 Hz, 1H), 6.94 (d, J = 8.8 Hz, 1H), 3.59–3.51 (m, 2H), 2.95 (t, J = 7.2 Hz, 2H). ^{13}C NMR (101 MHz, DMSO) δ 167.88 (s), 159.03 (s), 135.16 (s), 133.65 (s), 128.85 (s), 127.69 (s), 125.23 (s), 123.53 (s), 122.76 (s), 121.34 (s), 119.76 (s), 118.05 (s), 117.29 (s), 113.40

(s), 112.04 (s), 25.00 (s). MS (ESI): 349.21 ($C_{17}H_{14}Cl_2N_2O_2$, [M + H^+]).

5-Bromo-N-[2-(5-chloro-1H-indol-3-yl)-ethyl]-2-hydroxy-benzamide (E12). White powder, 75.47% yield, mp 182–185 °C. ^{1}H NMR (400 MHz, DMSO) δ 12.66 (s, 1H), 11.07 (s, 1H), 9.01 (t, J = 5.5 Hz, 1H), 8.04 (d, J = 2.4 Hz, 1H), 7.61 (d, J = 1.8 Hz, 1H), 7.54 (dd, J = 8.8, 2.4 Hz, 1H), 7.36 (d, J = 8.6 Hz, 1H), 7.28 (d, J = 2.1 Hz, 1H), 7.07 (dd, J = 8.6, 2.0 Hz, 1H), 6.89 (d, J = 8.8 Hz, 1H), 3.56 (dd, J = 13.1, 7.0 Hz, 2H), 2.96 (t, J = 7.2 Hz, 2H). ^{13}C NMR (101 MHz, acetone) δ 168.97 (s), 160.90 (s), 136.35 (s), 135.24 (s), 129.10 (s), 128.83 (s), 124.58 (s), 124.07 (s), 121.33 (s), 120.00 (s), 117.83 (s), 116.40 (s), 112.73 (s), 112.19 (s), 109.52 (s), 40.25 (s), 24.73 (s). MS (ESI): 393.66 ($C_{17}H_{14}BrClN_2O_2$, [M + H^+]).

2-Hydroxy-N-[2-(5-methyl-1H-indol-3-yl)-ethyl]-benzamide (E13). Brown powder, 78.46% yield, mp 156–158 °C. ^{1}H NMR (400 MHz, acetone) δ 12.78 (s, 1H), 9.74 (s, 1H), 8.11 (s, 1H), 7.58 (d, J = 8.0 Hz, 1H), 7.26 (s, 1H), 7.23 (s, 1H), 7.12 (d, J = 8.2 Hz, 1H), 7.02 (s, 1H), 6.81–6.76 (m, 1H), 6.75 (s, 1H), 6.68 (t, J = 7.6 Hz, 1H), 3.58 (dd, J = 13.5, 6.7 Hz, 2H), 2.92 (t, J = 7.2 Hz, 2H), 2.23 (s, 3H). ^{13}C NMR (101 MHz, acetone) δ 170.68 (s), 160.26 (s), 136.88 (s), 134.39 (s), 127.69 (s), 126.63 (s), 123.91 (s), 122.58 (s), 121.31 (s), 118.62 (s), 118.42 (s), 117.58 (s), 113.79 (s), 112.32 (s), 111.33 (s), 40.21 (s), 25.13 (s), 14.90 (s). MS (ESI): 294.35 ($C_{18}H_{18}N_2O_2$, [M + H^+]).

2-Hydroxy-3-methyl-N-[2-(5-methyl-1H-indol-3-yl)-ethyl]-benzamide (E14). Brown powder, 78.46% yield, mp 142–144 °C. ^{1}H NMR (400 MHz, DMSO) δ 12.75 (s, 1H), 10.67(s, 1H), 8.88 (t, J = 5.6 Hz, 1H), 7.74 (d, J = 8.0 Hz, 1H), 7.35 (s, 1H), 7.23 (d, J = 8.2 Hz, 1H), 7.13 (d, J = 2.2 Hz, 1H), 6.85 (dd, J = 8.3, 1.3 Hz, 1H), 6.71 (d, J = 6.1 Hz, 1H), 6.70 (s, 1H), 3.55 (dd, J = 13.3, 7.2 Hz, 2H), 2.94 (t, J = 7.4 Hz, 2H), 2.36 (s, 3H), 2.28 (s, 3H); ^{13}C NMR (101 MHz, acetone) δ 170.66 (s), 160.25 (s), 135.26 (s), 134.35 (s), 127.97 (s), 127.35 (s), 126.60 (s), 123.90 (s), 122.88 (s), 122.67 (s), 118.13 (s), 117.56 (s), 113.81 (s), 111.86 (s), 111.02 (s), 40.33 (s), 25.08 (s), 20.73 (s), 14.88 (s). MS (ESI): 308.37 ($C_{19}H_{20}N_2O_2$, [M + H^+]).

2-Hydroxy-4-methyl-N-[2-(5-methyl-1H-indol-3-yl)-ethyl]-benzamide (E15). Brown powder, 79.78% yield, mp 142–144 °C. ^{1}H NMR (400 MHz, DMSO) δ 12.73 (s, 1H), 10.69 (s, 1H), 8.86 (t, J = 5.6 Hz, 1H), 7.73 (d, J = 8.0 Hz, 1H), 7.34 (s, 1H), 7.23 (d, J = 8.2 Hz, 1H), 7.13 (d, J = 2.2 Hz, 1H), 6.89 (dd, J = 8.3, 1.3 Hz, 1H), 6.71 (d, J = 6.1 Hz, 1H), 6.70 (s, 1H), 3.55 (dd, J = 13.3, 7.2 Hz, 2H), 2.94 (t, J = 7.4 Hz, 2H), 2.36 (s, 3H), 2.28 (s, 3H). ^{13}C NMR (101 MHz, DMSO) δ 169.56 (s), 160.82 (s), 144.48 (s), 135.11 (s), 127.87 (d, J = 10.7 Hz), 127.09 (s), 123.25 (s), 123.00 (s), 119.97 (s), 118.38 (s), 117.98 (s), 112.93 (s), 111.58 (d, J = 3.9 Hz), 25.42 (s), 21.63 (d, J = 17.3 Hz). MS (ESI): 308.37 ($C_{19}H_{20}N_2O_2$, [M + H^+]).

4-Chloro-2-hydroxy-N-[2-(5-methyl-1H-indol-3-yl)-ethyl]-benzamide (E16). Brown powder, 75.38% yield, mp 152–154 °C. ^{1}H NMR (400 MHz, acetone) δ 13.27 (s, 1H), 9.90 (s, 1H), 8.34 (s, 1H), 7.75 (d, J = 8.5 Hz, 1H), 7.40 (s, 1H), 7.28 (d, J = 8.2 Hz, 1H), 7.17 (s, 1H), 6.96 (s, 1H), 6.94 (s, 1H), 6.87 (d, J = 8.5 Hz, 1H), 3.73 (q, J = 6.5 Hz, 2H), 3.07 (t, J = 7.2 Hz, 2H), 2.39 (s, 3H); ^{13}C NMR (101 MHz, acetone) δ 169.50 (s), 162.73 (s), 138.56 (s), 135.25 (s), 127.99 (d, J = 9.4 Hz), 127.37 (s), 122.81 (d, J = 18.3 Hz), 118.53 (s), 118.10 (s), 117.54 (s), 113.60 (s), 111.73 (s), 111.05 (s), 40.40 (s), 24.97 (s), 20.73 (s). MS (ESI): 328.79 ($C_{18}H_{17}ClN_2O_2$, [M + H^+]).

5-Chloro-2-hydroxy-N-[2-(5-methyl-1H-indol-3-yl)-ethyl]-benzamide (E17). Brown powder, 70.38% yield, mp 162–164 °C. ^{1}H NMR (400 MHz, acetone) δ 12.93 (s, 1H), 9.91 (s, 1H), 8.38 (s, 1H), 7.78 (s, 1H), 7.42 (s, 1H), 7.40 (s, 1H), 7.28 (d, J = 8.2 Hz, 1H), 7.18 (s, 1H,), 6.95 (d, J = 3.8 Hz, 1H), 6.93 (s, 1H), 3.74 (q, J = 6.5 Hz, 2H), 3.08 (t, J = 7.2 Hz, 2H), 2.39 (s, 3H); ^{13}C NMR (101 MHz, acetone) δ 169.01 (s), 160.50 (s), 135.24 (s), 133.45 (s), 127.96 (s), 127.40 (s), 126.19 (s), 122.73 (t, J = 18.4 Hz), 119.56 (s), 118.11 (s), 115.85 (s), 111.77 (s), 111.05 (s), 40.54 (s), 24.93 (s), 20.73 (s). MS (ESI): 328.79 ($C_{18}H_{17}ClN_2O_2$, [M + H^+]).

5-Bromo-2-hydroxy-N-[2-(5-methyl-1H-indol-3-yl)-ethyl]-benzamide (E18). Brown powder, 72.34% yield, mp 161–163 °C. ^{1}H NMR (400 MHz, acetone) δ 12.97 (s, 1H), 9.91 (s, 1H), 8.40 (s, 1H), 7.90 (s, 1H), 7.54 (d, J = 8.8 Hz, 1H), 7.40 (s, 1H), 7.28 (d, J = 8.3 Hz, 1H), 7.17 (s, 1H), 6.95 (d, J = 8.2 Hz, 1H), 6.89 (d, J = 8.8 Hz, 1H), 3.74 (q, J = 6.5 Hz, 2H), 3.08 (t, J = 7.1 Hz, 2H), 2.39 (s, 3H); ^{13}C NMR (101 MHz, acetone) δ 170.21 (s), 161.89 (s), 135.26 (s), 133.73 (s), 127.97 (s), 127.37 (s), 126.52 (s), 122.90 (s), 122.70 (s), 118.20 (d, J = 10.9 Hz), 117.81 (s), 114.73 (s), 111.85 (s), 111.05 (s), 40.33 (s), 25.09 (s), 20.75 (s). MS (ESI): 373.24 ($C_{18}H_{17}BrN_2O_2$, [M + H^+]).

N-[2-(5-Bromo-1H-indol-3-yl)-ethyl]-2-hydroxy benzamide (E19). Brown powder, 79.38% yield, mp 124–126 °C. ^{1}H NMR (400 MHz, DMSO) δ 12.63 (d, J = 4.5 Hz, 1H), 11.06 (s, 1H), 8.94 (t, J = 5.6 Hz, 1H), 7.83 (dd, J = 7.9, 1.3 Hz, 1H), 7.77 (d, J = 1.8 Hz, 1H), 7.42–7.37 (m, 1H), 7.32 (d, J = 8.6 Hz, 1H), 7.26 (d, J = 2.3 Hz, 1H), 7.18 (dd, J = 8.6, 1.9 Hz, 1H), 6.91 (s, 1H), 6.89–6.86 (m, 1H), 3.56 (dd, J = 13.2, 7.1 Hz, 2H), 3.01–2.90 (m, 2H). ^{13}C NMR (101 MHz, DMSO) δ 169.38 (s), 160.57 (s), 135.39 (s), 134.08 (s), 129.59 (s), 128.08 (s), 125.02 (s), 123.85 (s), 121.10 (s), 119.00 (s), 117.84 (s), 115.69 (s), 113.88 (s), 112.04 (s), 111.47 (s), 25.13 (s). MS (ESI): 359.22 ($C_{17}H_{15}BrN_2O_2$, [M + H^+]).

N-[2-(5-Bromo-1H-indol-3-yl)-ethyl]-2-hydroxy-3-methyl-benzamide (E20). Brown powder, 80.23% yield, mp 183–185 °C. ^{1}H NMR (400 MHz, DMSO) δ 13.27 (s, 1H), 11.06 (s, 1H), 8.99 (t, J = 5.6 Hz, 1H), 7.76 (d, J = 1.8 Hz, 1H), 7.65 (d, J = 7.2 Hz, 1H), 7.32 (d, J = 8.6 Hz, 1H), 7.29 (s, 1H), 7.26 (d, J = 2.3 Hz, 1H), 7.18 (dd, J = 8.6, 1.9 Hz, 1H), 6.78 (t, J = 7.7 Hz, 1H), 3.55 (dd, J = 13.2, 7.1 Hz, 2H), 2.96 (t, J = 7.3 Hz, 2H), 2.16 (s, 3H). ^{13}C NMR (101 MHz, DMSO) δ 170.57 (s), 159.83 (s), 135.37 (s), 134.89 (s), 129.59 (s), 126.43 (s), 124.96 (d, J = 11.6 Hz), 123.84 (s), 121.07 (s), 118.13 (s), 113.93 (d, J = 9.2 Hz), 112.01 (s), 111.47 (s), 25.05 (s), 15.93 (s). MS (ESI): 373.24 ($C_{18}H_{17}BrN_2O_2$, [M + H^+]).

N-[2-(5-Bromo-1H-indol-3-yl)-ethyl]-2-hydroxy-4-methyl-benzamide (E21). Brown powder, 75.23% yield, mp 135–137 °C. ^{1}H NMR (400 MHz, DMSO) δ 12.68 (s, 1H), 11.06 (s, 1H), 8.85 (t, J = 5.6 Hz, 1H), 7.77 (d, J = 1.8 Hz, 1H), 7.72 (d, J = 8.4 Hz, 1H), 7.32 (d, J = 8.6 Hz, 1H), 7.26 (d, J = 2.2 Hz, 1H), 7.18 (dd, J = 8.6, 1.9 Hz, 1H), 6.72 (s, 1H), 6.70 (s, 1H), 3.54 (dd, J

= 13.3, 7.1 Hz, 2H), 2.95 (t, *J* = 7.3 Hz, 2H), 2.27 (s, 3H). ^{13}C NMR (101 MHz, DMSO) δ 169.56 (s), 160.78 (s), 144.51 (s), 135.38 (s), 129.59 (s), 127.80 (s), 124.99 (s), 123.85 (s), 121.10 (s), 120.01 (s), 117.99 (s), 113.88 (s), 112.90 (s), 112.06 (s), 111.47 (s), 25.16 (s), 21.55 (s). MS (ESI): 373.24 ($C_{18}H_{17}BrN_2O_2$, [M + H$^+$]).

N-[2-(5-Bromo-1H-indol-3-yl)-ethyl]-4-chloro-2-hydroxybenzamide (E22). Brown powder, 72.23% yield, mp 143–144 °C. ^{1}H NMR (400 MHz, DMSO) δ 12.92 (s, 1H), 11.06 (s, 1H), 8.96 (t, *J* = 5.6 Hz, 1H), 7.85 (d, *J* = 8.4 Hz, 1H), 7.75 (d, *J* = 1.9 Hz, 1H), 7.32 (d, *J* = 8.6 Hz, 1H), 7.26 (d, *J* = 2.3 Hz, 1H), 7.17 (dd, *J* = 8.6, 1.9 Hz, 1H), 6.99 (d, *J* = 1.5 Hz, 1H), 6.96 (d, *J* = 2.1 Hz, 1H), 3.55 (dd, *J* = 13.1, 7.1 Hz, 2H), 2.95 (t, *J* = 7.3 Hz, 2H). ^{13}C NMR (101 MHz, DMSO) δ 168.39 (s), 161.20 (s), 137.99 (s), 135.39 (s), 129.91 (s), 129.57 (s), 125.05 (s), 123.85 (s), 121.10 (s), 119.29 (s), 117.47 (s), 115.01 (s), 113.88 (s), 111.98 (s), 111.48 (s), 25.04 (s). MS (ESI): 393.66 ($C_{17}H_{14}BrClN_2O_2$, [M + H$^+$]).

N-[2-(5-Bromo-1H-indol-3-yl)-ethyl]-5-chloro-2-hydroxybenzamide (E23). Brown powder, 70.23% yield, mp 161–164 °C. ^{1}H NMR (400 MHz, DMSO) δ 12.61 (s, 1H), 11.06 (s, 1H), 8.99 (t, *J* = 5.5 Hz, 1H), 7.91 (d, *J* = 2.6 Hz, 1H), 7.75 (d, *J* = 1.8 Hz, 1H), 7.43 (dd, *J* = 8.8, 2.6 Hz, 1H), 7.32 (d, *J* = 8.6 Hz, 1H), 7.27 (d, *J* = 2.2 Hz, 1H), 7.18 (dd, *J* = 8.6, 1.9 Hz, 1H), 6.94 (d, *J* = 8.8 Hz, 1H), 3.55 (dd, *J* = 13.1, 7.1 Hz, 2H), 2.95 (t, *J* = 7.2 Hz, 2H). ^{13}C NMR (101 MHz, DMSO) δ 167.89 (s), 159.04 (s), 135.39 (s), 133.65 (s), 129.57 (s), 127.69 (s), 125.08 (s), 123.86 (s), 122.77 (s), 121.09 (s), 119.77 (s), 117.28 (s), 113.89 (s), 111.98 (s), 111.49 (s), 24.98 (s). MS (ESI): 393.66 ($C_{17}H_{14}BrClN_2O_2$, [M + H$^+$]).

5-Bromo-N-[2-(5-bromo-1H-indol-3-yl)-ethyl]-2-hydroxybenzamide (E24). White powder, 71.23% yield, mp 152–154 °C. ^{1}H NMR (400 MHz, DMSO) δ 12.63 (d, *J* = 4.9 Hz, 1H), 11.06 (s, 1H), 8.99 (t, *J* = 5.5 Hz, 1H), 8.03 (d, *J* = 2.5 Hz, 1H), 7.75 (d, *J* = 1.8 Hz, 1H), 7.54 (dd, *J* = 8.8, 2.5 Hz, 1H), 7.32 (d, *J* = 8.6 Hz, 1H), 7.26 (d, *J* = 2.2 Hz, 1H), 7.18 (dd, *J* = 8.6, 1.9 Hz, 1H), 6.89 (d, *J* = 8.8 Hz, 1H), 3.55 (dd, *J* = 13.1, 7.1 Hz, 2H), 2.95 (t, *J* = 7.2 Hz, 2H). ^{13}C NMR (101 MHz, DMSO) δ 167.84 (s), 159.47 (s), 136.46 (s), 135.39 (s), 130.56 (s), 129.57 (s), 125.07 (s), 123.86 (s), 121.09 (s), 120.20 (s), 117.83 (s), 113.89 (s), 111.98 (s), 111.49 (s), 110.20 (s), 24.98 (s). MS (ESI): 438.11 ($C_{17}H_{14}Br_2N_2O_2$, [M + H$^+$]).

N-(2-(5-Fluoro-1H-indol-3-yl)ethyl)-2-hydroxybenzamide (E25). White powder, 78.23% yield, mp 117–120 °C. ^{1}H NMR (400 MHz, DMSO) δ 12.65 (s, 1H), 10.94 (s, 1H), 8.94 (t, *J* = 5.5 Hz, 1H), 7.84 (dd, *J* = 7.9, 1.5 Hz, 1H), 7.42–7.37 (m, 1H), 7.35 (d, *J* = 4.1 Hz, 1H), 7.34–7.31 (m, 1H), 7.28 (d, *J* = 2.2 Hz, 1H), 6.94 (d, *J* = 2.5 Hz, 1H), 6.91 (s, 1H), 6.89 (d, *J* = 1.5 Hz, 1H), 3.57 (dd, *J* = 13.3, 7.2 Hz, 2H), 2.95 (t, *J* = 7.4 Hz, 2H). ^{13}C NMR (101 MHz, DMSO) δ 169.38 (s), 160.56 (s), 158.29 (s), 156.00 (s), 134.08 (s), 133.37 (s), 128.32–127.77 (m), 125.38 (s), 118.98 (s), 117.85 (s), 115.71 (s), 112.78 (d, *J* = 9.8 Hz), 112.41 (d, *J* = 4.8 Hz), 109.64 (s), 109.38 (s), 103.52 (s), 103.29 (s), 25.26 (s). MS (ESI): 298.11 ($C_{17}H_{15}FN_2O_2$, [M + H$^+$]).

N-(2-(5-Fluoro-1H-indol-3-yl)ethyl)-2-hydroxy-3-methylbenzamide (E26). White powder, 79.43% yield, mp 147–149 °C. ^{1}H NMR (400 MHz, DMSO) δ 13.30 (s, 1H), 10.94 (s, 1H), 8.99 (t, *J* = 5.6 Hz, 1H), 7.67 (dd, *J* = 5.9, 2.1 Hz, 1H), 7.35 (s, 1H), 7.34 (d, *J* = 3.9 Hz, 1H), 7.32–7.30 (m, 1H), 7.28 (d, *J* = 2.3 Hz, 1H), 6.91 (td, *J* = 9.3, 2.5 Hz, 1H), 6.78 (t, *J* = 7.7 Hz, 1H), 3.56 (dd, *J* = 13.3, 7.2 Hz, 2H), 2.95 (t, *J* = 7.4 Hz, 2H), 2.16 (s, 3H). ^{13}C NMR (101 MHz, DMSO) δ 170.59 (s), 159.85 (s), 134.89 (s), 133.36 (s), 126.44 (s), 125.37 (s), 124.90 (s), 118.11 (s), 112.78 (d, *J* = 9.8 Hz), 112.38 (d, *J* = 4.8 Hz), 109.63 (s), 109.37 (s), 103.48 (s), 103.25 (s), 25.19 (s), 15.92 (s). MS (ESI): 312.34 ($C_{18}H_{17}FN_2O_2$, [M + H$^+$]).

N-(2-(5-Fluoro-1H-indol-3-yl)ethyl)-2-hydroxy-4-methylbenzamide (E27). White powder, 79.43% yield, mp 144–148 °C. ^{1}H NMR (400 MHz, DMSO) δ 12.69 (s, 1H), 10.94 (s, 1H), 8.86 (t, *J* = 5.6 Hz, 1H), 7.72 (d, *J* = 8.0 Hz, 1H), 7.34 (dd, *J* = 5.1, 3.6 Hz, 1H), 7.32 (d, *J* = 2.2 Hz, 1H), 7.27 (d, *J* = 2.2 Hz, 1H), 6.91 (td, *J* = 9.2, 2.5 Hz, 1H), 6.72 (s, 1H), 6.70 (s, 1H), 3.55 (dd, *J* = 13.3, 7.2 Hz, 2H), 2.94 (t, *J* = 7.4 Hz, 2H), 2.27 (s, 3H). ^{13}C NMR (101 MHz, DMSO) δ 169.55 (s), 160.77 (s), 144.51 (s), 133.36 (s), 127.81 (s), 125.36 (s), 120.00 (s), 117.99 (s), 112.77 (d, *J* = 9.9 Hz), 112.43 (d, *J* = 4.8 Hz), 109.63 (s), 109.37 (s), 103.51 (s), 103.28 (s), 25.28 (s), 21.54 (s). MS (ESI): 312.34 ($C_{18}H_{17}FN_2O_2$, [M + H$^+$]).

4-Chloro-N-(2-(5-fluoro-1H-indol-3-yl)ethyl)-2-hydroxybenzamide (E28). White powder, 75.54% yield, mp 175–180 °C. ^{1}H NMR (400 MHz, DMSO) δ 12.93 (s, 1H), 10.94 (s, 1H), 8.97 (t, *J* = 5.5 Hz, 1H), 7.87 (d, *J* = 8.4 Hz, 1H), 7.36–7.33 (m, 1H), 7.32–7.30 (m, 1H), 7.27 (d, *J* = 2.2 Hz, 1H), 6.99 (dd, *J* = 3.7, 2.0 Hz, 1H), 6.96 (d, *J* = 2.1 Hz, 1H), 6.91 (td, *J* = 9.2, 2.5 Hz, 1H), 3.57 (dd, *J* = 13.2, 7.2 Hz, 2H), 2.94 (t, *J* = 7.3 Hz, 2H). ^{13}C NMR (101 MHz, DMSO) δ 168.37 (s), 161.20 (s), 137.99 (s), 133.37 (s), 129.92 (s), 125.41 (s), 119.28 (s), 117.47 (s), 112.78 (d, *J* = 9.8 Hz), 112.33 (d, *J* = 4.8 Hz), 109.64 (s), 109.39 (s), 103.51 (s), 103.28 (s), 25.17 (s). MS (ESI): 332.76 ($C_{17}H_{14}ClFN_2O_2$, [M + H$^+$]).

5-Chloro-N-(2-(5-fluoro-1H-indol-3-yl)ethyl)-2-hydroxybenzamide (E29). White powder, 70.54% yield, mp 170–172 °C. ^{1}H NMR (400 MHz, DMSO) δ 12.61 (s, 1H), 10.95 (s, 1H), 8.99 (t, *J* = 5.4 Hz, 1H), 7.93 (d, *J* = 2.6 Hz, 1H), 7.43 (dd, *J* = 8.8, 2.6 Hz, 1H), 7.34 (t, *J* = 4.3 Hz, 1H), 7.32 (d, *J* = 3.6 Hz, 1H), 7.28 (d, *J* = 2.2 Hz, 1H), 6.96–6.92 (m, 1H), 6.90 (dd, *J* = 9.1, 2.4 Hz, 1H), 3.57 (dd, *J* = 13.2, 7.1 Hz, 2H), 2.94 (t, *J* = 7.3 Hz, 2H). ^{13}C NMR (101 MHz, DMSO) δ 167.86 (s), 159.02 (s), 133.64 (s), 133.37 (s), 127.71 (s), 125.43 (s), 119.76 (s), 117.32 (s), 112.79 (d, *J* = 9.8 Hz), 112.31 (d, *J* = 4.7 Hz), 109.65 (s), 109.39 (s), 103.50 (s), 103.28 (s), 25.11 (s). MS (ESI): 332.76 ($C_{17}H_{14}ClFN_2O_2$, [M + H$^+$]).

5-Bromo-N-(2-(5-fluoro-1H-indol-3-yl)ethyl)-2-hydroxybenzamide (E30). White powder, 71.54% yield, mp 176–179 °C. ^{1}H NMR (400 MHz, DMSO) δ 12.64 (s, 1H), 10.95 (s, 1H), 8.99 (t, *J* = 5.5 Hz, 1H), 8.04 (d, *J* = 2.5 Hz, 1H), 7.54 (dd, *J* = 8.8, 2.5 Hz, 1H), 7.36–7.33 (m, 1H), 7.32–7.30 (m, 1H), 7.28 (d, *J* = 2.2 Hz, 1H), 6.92–6.90 (m, 1H), 6.90–6.87 (m, 1H), 3.56 (dd, *J* = 13.1, 7.1 Hz, 2H), 2.94 (t, *J* = 7.3 Hz, 2H). ^{13}C NMR (101 MHz, DMSO) δ 167.81 (s), 159.45 (s), 136.45 (s), 133.37

(s), 130.58 (s), 125.43 (s), 120.20 (s), 117.86 (s), 112.79 (d, J = 9.7 Hz), 112.31 (d, J = 4.8 Hz), 109.65 (s), 109.39 (s), 103.50 (s), 103.27 (s), 25.11 (s). MS (ESI): 377.21 ($C_{17}H_{14}BrFN_2O_2$, [M + H^+]).

2-Hydroxy-N-(2-(5-methoxy-1H-indol-3-yl)ethyl)benzamide (E31). White powder, 70.34% yield, mp 125–127 °C. ^{1}H NMR (400 MHz, $CDCl_3$) δ 12.40 (s, 1H), 8.07 (s, 1H), 7.32 (d, J = 8.8 Hz, 2H), 7.29 (s, 1H), 7.10 (d, J = 2.6 Hz, 2H), 6.96–6.93 (m, 1H), 6.93–6.91 (m, 1H), 6.41 (s, 1H), 3.84 (s, 3H), 3.78 (dd, J = 12.4, 6.3 Hz, 2H), 3.09 (t, J = 6.5 Hz, 2H). ^{13}C NMR (101 MHz, $CDCl_3$) δ 169.91 (s), 161.57 (s), 154.23 (s), 134.16 (s), 131.54 (s), 127.65 (s), 125.31 (s), 122.93 (s), 118.59 (d, J = 2.8 Hz), 114.28 (s), 112.76 (s), 112.48 (s), 112.19 (s), 100.26 (s), 55.81 (s), 40.04 (s), 25.11 (s). MS (ESI): 310.35 ($C_{18}H_{18}N_2O_3$, [M + H^+]).

2-Hydroxy-N-(2-(5-methoxy-1H-indol-3-yl)ethyl)-3-methylbenzamide (E32). White powder, 69.34% yield, mp 125–127 °C. ^{1}H NMR (400 MHz, $CDCl_3$) δ 12.74 (s, 1H), 8.04 (s, 1H), 7.32 (s, 1H), 7.29 (d, J = 3.6 Hz, 2H), 7.25 (d, J = 7.3 Hz, 1H), 6.98 (d, J = 7.8 Hz, 1H), 6.91 (dd, J = 8.8, 2.3 Hz, 1H), 6.68 (t, J = 7.6 Hz, 1H), 6.44 (s, 1H), 3.81 (s, 3H), 3.80–3.76 (m, 2H), 3.09 (t, J = 6.5 Hz, 2H), 2.28 (s, 3H). ^{13}C NMR (101 MHz, $CDCl_3$) δ 170.32 (s), 160.00 (s), 154.23 (s), 134.84 (s), 131.52 (s), 127.64 (s), 122.83 (d, J = 13.8 Hz), 117.87 (s), 113.44 (s), 112.77 (s), 112.54 (s), 112.16 (s), 100.27 (s), 55.81 (s), 40.01 (s), 25.14 (s), 15.82 (s). MS (ESI): 324.37 ($C_{19}H_{20}N_2O_3$, [M + H^+]).

2-Hydroxy-N-(2-(5-methoxy-1H-indol-3-yl)ethyl)-4-methylbenzamide (E33). White powder, 68.04% yield, mp 125–127 °C. ^{1}H NMR (400 MHz, $CDCl_3$) δ 12.48 (s, 1H), 8.08 (s, 1H), 7.29 (d, J = 1.7 Hz, 1H), 7.06 (s, 2H), 7.01 (d, J = 8.1 Hz, 1H), 6.91 (dd, J = 8.8, 2.4 Hz, 1H), 6.81 (s, 1H), 6.58 (d, J = 8.1 Hz, 1H), 6.41 (s, 1H), 3.81 (s, 3H), 3.79–3.75 (m, 2H), 3.08 (t, J = 6.5 Hz, 2H), 2.32 (s, 3H). ^{13}C NMR (101 MHz, $CDCl_3$) δ 169.94 (s), 161.55 (s), 154.21 (s), 145.21 (s), 131.53 (s), 127.67 (s), 125.15 (s), 122.92 (s), 119.77 (s), 118.69 (s), 112.64 (d, J = 19.5 Hz), 112.17 (s), 111.66 (s), 100.26 (s), 55.80 (s), 39.98 (s), 25.15 (s), 21.61 (s). MS (ESI): 324.37 ($C_{19}H_{20}N_2O_3$, [M + H^+]).

4-Chloro-2-hydroxy-N-(2-(5-methoxy-1H-indol-3-yl)ethyl)-benzamide (E34). White powder, 68.04% yield, mp 128–132 °C. ^{1}H NMR (400 MHz, $CDCl_3$) δ 12.70 (s, 1H), 8.09 (s, 1H), 7.31 (s, 1H), 7.29 (d, J = 2.6 Hz, 1H), 7.07–7.03 (m, 2H), 7.02–6.99 (m, 1H), 6.92 (dd, J = 8.8, 2.4 Hz, 1H), 6.74 (dd, J = 8.5, 2.0 Hz, 1H), 6.41 (s, 1H), 3.82 (s, 3H), 3.79–3.75 (m, 2H), 3.08 (t, J = 6.5 Hz, 2H). ^{13}C NMR (101 MHz, $CDCl_3$) δ 169.25 (s), 162.33 (s), 154.24 (s), 139.66 (s), 131.55 (s), 127.62 (s), 126.31 (s), 122.95 (s), 119.06 (s), 118.60 (s), 112.78 (d, J = 9.7 Hz), 112.28 (d, J = 8.2 Hz), 100.27 (s), 55.84 (s), 40.11 (s), 25.01 (s). MS (ESI): 344.79 ($C_{18}H_{17}ClN_2O_3$, [M + H^+]).

5-Chloro-2-hydroxy-N-(2-(5-methoxy-1H-indol-3-yl)ethyl)-benzamide (E35). White powder, 68.22% yield, mp 131–135 °C. ^{1}H NMR (400 MHz, $CDCl_3$) δ 12.51 (s, 1H), 8.08 (s, 1H), 7.41–7.35 (m, 1H), 7.32 (s, 1H), 7.29 (d, J = 3.5 Hz, 1H), 7.13 (dd, J = 8.0, 1.2 Hz, 1H), 7.00 (d, J = 7.9 Hz, 1H), 6.91 (dd, J = 8.8, 2.4 Hz, 1H), 6.78 (dd, J = 11.2, 4.0 Hz, 1H), 6.47 (s, 1H), 3.81 (d, J = 4.1 Hz, 3H), 3.78 (d, J = 6.3 Hz, 2H), 3.09 (t, J = 6.5 Hz, 2H). ^{13}C NMR (101 MHz, $CDCl_3$) δ 168.82 (s), 160.11 (s), 154.32 (s), 133.99 (s), 131.54 (s), 127.59 (s), 124.99 (s), 123.24 (s), 122.90 (s), 120.07 (s), 115.22 (s), 112.76 (s), 112.25 (s), 100.23 (s), 55.83 (s), 40.21 (s), 29.73 (s), 24.99 (s). MS (ESI): 344.79 ($C_{18}H_{17}ClN_2O_3$, [M + H^+]).

5-Bromo-2-hydroxy-N-(2-(5-methoxy-1H-indol-3-yl)ethyl)-benzamide (E36). White powder, 68.34% yield, mp 139–142 °C. ^{1}H NMR (400 MHz, $CDCl_3$) δ 12.43 (s, 1H), 8.09 (d, J = 15.9 Hz, 1H), 7.45 (dd, J = 8.8, 2.3 Hz, 1H), 7.32 (d, J = 8.8 Hz, 1H), 7.28 (s, 1H), 7.23 (d, J = 2.3 Hz, 1H), 7.06 (d, J = 2.3 Hz, 1H), 6.93 (dd, J = 8.8, 2.4 Hz, 1H), 6.89 (d, J = 8.8 Hz, 1H), 6.41 (s, 1H), 3.84 (s, 3H), 3.77 (q, J = 6.4 Hz, 2H), 3.09 (t, J = 6.6 Hz, 2H). ^{13}C NMR (101 MHz, $CDCl_3$) δ 168.73 (s), 160.56 (s), 154.31 (s), 136.81 (s), 131.53 (s), 127.98 (s), 127.59 (s), 122.90 (s), 120.48 (s), 115.86 (s), 112.78 (s), 112.25 (s), 110.14 (s), 100.20 (s), 55.85 (s), 40.25 (s), 24.98 (s). MS (ESI): 389.24 ($C_{18}H_{17}BrN_2O_3$, [M + H^+]).

4.2 Biological evaluation

4.2.1 Cell culture. The human lung adenocarcinoma epithelial cell line (A549), human cervix adenocarcinoma cell line (HeLa), human gastric cancer cell line (MGC-803), human hepatoma cell line (HepG-2) and human breast cancer cell line (MCF-7) were purchased from the Type Culture Collection of the Chinese Academy of Sciences, Shanghai, China. Cells were grown in Dulbecco's Modified Eagle's Medium (DMEM, Gibco, NY, USA) mixed with 10% fetal bovine serum (Gibco, NY, USA), and all the cells were cultured in a 5% CO_2 incubator at 37 °C.

4.2.2 MTT. Cells were transplanted into 96-well plates at a density of 6000 cells per well and placed in the incubator for 24 h. For each assay, **E20** at five different concentrations (128, 64, 32, 16, and 8 μmol L^{-1}) and one control (3‰ DMSO) were added to six different wells and placed in the incubator for 48 h. After 48 h, MTT solution (20 μL) was added to each well and the plate was placed in the incubator for 4 h. Formazan was dissolved in 150 μL of DMSO. The absorbance (optical density, OD) was monitored on a Wellscan MK-2 microplate reader (LabSystems) at 490 nm. The IC_{50} values of each compound were calculated by Graph Pad Pro 5.0. The assay was performed three times.

4.2.3 Cell migration assay. MGC-803 cells were transplanted into 6-well plates at a density of 1×10^5 cells per well for 24 h. We scratched the cell culture with a 200 μL sterile pipette tip, then removed the floating cells with phosphate-buffered saline (PBS) and treated the cell culture with different concentrations of **E20** and the control group (3‰ DMSO) for 48 h. We captured images of the cells with a microscopic camera system at the time of treatment (0 h) and after 48 h to assess the re-growth of the colony back into the damaged region. The assay was performed three times.

4.2.4 Analysis of cellular apoptosis. MGC-803 cells (1×10^5 cells per well) were transplanted into 6-well plates and incubated for 24 h. Then the cells were treated with different concentrations of **E20** for 24 h and the control group was treated

with 3‰ DMSO. The cells were collected by trypsin digestion and washed twice at 4 °C with PBS. Then after centrifugation at 1200 rpm and removal of the supernatants, the cells were mixed with 400 μL of 1× binding buffer, 5 μL of Annexin V-FITC and 5 μL of propidium iodide (PI) (BD Pharmingen, USA), and incubated at 25 °C for 15 min in the dark. The stained cells were analyzed by flow cytometry. The assay was performed three times.

4.2.5 Colony formation assay. MGC-803 cells (1000 cells per well) were placed in 6-well plates and placed in the incubator for 24 h. They were then treated with different concentrations of **E20** and left in the incubator for 9 d, where the culture medium was changed every 3 d. At the end of the experiment the culture medium was removed, and the cells washed twice with PBS, immobilized with 4% paraformaldehyde for 20 min, stained with crystal violet for 15 min and washed with PBS. The assay was performed three times.

4.2.6 Cell cycle analysis. MGC-803 cells (1×10^5 cells per well) were incubated in 6-well plates for 24 h and treated with different concentrations of **E20** (20, 40, and 60 μmol L^{-1}) for 24 h and the control group was treated with 3‰ DMSO. After this time period, the culture medium was removed and the cells were washed twice with PBS, transferred to a centrifuge tube and centrifuged (1200 rpm). The cells were then washed at 4 °C with PBS and immobilized with 70% ethanol solution for 12 h at 4 °C. Then the cells were mixed with RNase A and propidium iodide staining solution (Beyotime, China). Flow cytometry was used to analyze the cells. The assay was performed three times.

4.2.7 Western blot. MGC-803 cells (1×10^5 cells per well) were placed in 6-well plates for 24 h and treated with different concentrations of **E20** (10, 20, and 40 μmol L^{-1}) for 24 h. The expression of HIF-1α was investigated under $CoCl_2$ treatment (100 μM) and serum starvation (0.1% FBS)[25] in order to create the hypoxia environment. Protein expression was analyzed by western blotting as described elsewhere[26] (Image J2x). The assay was performed three times.

Conflicts of interest

The authors declare that there are no conflicts of interest.

Acknowledgements

This work was financially supported by Hunan Province Cooperative Innovation Center for Molecular Target New Drug Study (0223-0002-0002000-49), Innovation Platform Open Foundation of the Education, Department of Hunan province (contract grant number 16K079, 17K082) and Graduate Student Science Foundation of the University of South China (2018490).

References

1 J. Leon, D. Acuña-Castroviejo, R. M. Sainz, J. C. Mayo, D. X. Tan and R. J. Reiter, *Life Sci.*, 2004, **75**, 765–790.
2 O. Pechanova, L. Paulis and F. Simko, *Int. J. Mol. Sci.*, 2014, **15**, 17920–17937.
3 J. R. Calvo, C. Gonzálezyanes and M. D. Maldonado, *J. Pineal Res.*, 2013, **55**, 103–120.
4 J. Barrenetxe, P. Delagrange and J. A. Martínez, *J. Physiol. Biochem.*, 2004, **60**, 61–72.
5 M. Karasek, *Exp. Gerontol.*, 2004, **39**, 1723–1729.
6 V. Alvarez-García, A. González, C. Alonso-González, C. Martínez-Campa and S. Cos, *J. Pineal Res.*, 2013, **54**, 373–380.
7 W. Li, M. Fan, Y. Chen, Q. Zhao, C. Song, Y. Yan, Y. Jin, Z. Huang, C. Lin and J. Wu, *Cell. Physiol. Biochem.*, 2015, **37**, 2323–2338.
8 L. Fan, G. Sun, T. Ma, F. Zhong, Y. Lei, X. Li and W. Wei, *J. Pineal Res.*, 2013, **55**, 184–194.
9 J. Song, S. J. Ma, J. H. Luo, H. Zhang, R. X. Wang, H. Liu, L. Li, Z. G. Zhang and R. X. Zhou, *Oncol. Rep.*, 2018, **39**, 1975.
10 L. Mao, R. T. Dauchy, D. E. Blask, E. M. Dauchy, L. M. Slakey, S. Brimer, L. Yuan, S. Xiang, A. Hauch, K. Smith, T. Frasch, V. P. Belancio, M. A. Wren and S. M. Hill, *J. Pineal Res.*, 2016, **60**, 167–177.
11 N. H. Goradel, M. H. Asghari, M. Moloudizargari, B. Negahdari, H. Haghi-Aminjan and M. Abdollahi, *Toxicol. Appl. Pharmacol.*, 2017, **335**, 56–63.
12 G. Gatti, V. Lucini, S. Dugnani, A. Calastretti, G. Spadoni, A. Bedini, S. Rivara, M. Mor, G. Canti and F. Scaglione, *Oncotarget*, 2017, **8**, 68338–68353.
13 A. Calastretti, G. Gatti, V. Lucini, S. Dugnani, G. Canti, F. Scaglione and A. Bevilacqua, *Int. J. Mol. Sci.*, 2018, **19**(5), 1505.
14 R. Silvia, P. Daniele, B. Annalida and S. Gilberto, *Expert Opin. Ther. Pat.*, 2015, **25**, 1–17.
15 M. J. Thun, E. J. Jacobs and C. Patrono, *Nat. Rev. Clin. Oncol.*, 2012, **9**, 259–267.
16 M. Jin, C. Li, Q. Zhang, S. Xing, X. Kan and J. Wang, *Oncol. Lett.*, 2018, **15**, 8454–8460.
17 R. Pathirana, P. West, D. Hedderley and J. Eason, *Protoplasma*, 2017, **254**, 1–13.
18 G. A. Spitz, C. M. Furtado, M. Sola-Penna and P. Zancan, *Biochem. Pharmacol.*, 2009, **77**, 46–53.
19 R. Hanif, A. Pittas, Y. Feng, M. I. Koutsos, L. Qiao, L. Staiano-Coico, S. I. Shiff and B. Rigas, *Biochem. Pharmacol.*, 1996, **52**, 237.
20 L. M. Green, J. L. Reade and C. F. Ware, *J. Immunol. Methods*, 1984, **70**, 257–268.
21 J. W. Astin, J. Batson, S. Kadir, J. Charlet, R. A. Persad, D. Gillatt, J. D. Oxley and C. D. Nobes, *Nat. Cell Biol.*, 2010, **12**, 1194–1204.
22 R. Z. Huang, G. B. Liang, X. C. Huang, B. Zhang, M. M. Zhou, Z. X. Liao and H. S. Wang, *Eur. J. Med. Chem.*, 2017, **138**, 979.
23 S. J. Martin, C. P. Reutelingsperger, A. J. Mcgahon, J. A. Rader, R. C. V. Schie, D. M. Laface and D. R. Green, *J. Exp. Med.*, 1995, **182**, 1545–1556.
24 C. Granchi and F. Minutolo, *ChemMedChem*, 2012, **7**, 1318–1350.
25 Z. Wen, C. Huang, Y. Xu, Y. Xiao, L. Tang, J. Dai, H. Sun, B. Chen and M. Zhou, *Eur. J. Pharmacol.*, 2016, **771**, 93–98.
26 L. Tao, L. Wei, Y. Liu, Y. Ding, X. Liu, X. Zhang, X. Wang, Y. Yao, J. Lu and Q. Wang, *Biochem. Pharmacol.*, 2016, **125**, 12–25.